

PAPER • OPEN ACCESS

Status update on SUNDAE2 magnetic field test facility at European XFEL

To cite this article: J E Baader *et al* 2024 *J. Phys.: Conf. Ser.* **2687** 032044

View the [article online](#) for updates and enhancements.

You may also like

- [Methods for calibrating the gain and offset of the DSSC detector for the European XFEL using X-ray line sources](#)
S. Schlee, G. Weidenspointner, D. Moch et al.
- [AMO science at the FLASH and European XFEL free-electron laser facilities](#)
J Feldhaus, M Krikunova, M Meyer et al.
- [Current status and future perspectives of accelerator-based x-ray light sources](#)
Takashi Tanaka



PRIME
PACIFIC RIM MEETING
ON ELECTROCHEMICAL
AND SOLID STATE SCIENCE

HONOLULU, HI
Oct 6–11, 2024

Abstract submission deadline:
April 12, 2024

Learn more and submit!



Joint Meeting of

The Electrochemical Society
•
The Electrochemical Society of Japan
•
Korea Electrochemical Society

Status update on SUNDAE2 magnetic field test facility at European XFEL

J E Baader¹, S Abeghyan¹, L Alanakyan¹, S Casalbuoni¹, D La Civita¹, U Englisch¹, B Marchetti¹, G Yakopov¹, M Yakopov¹, P Ziolkowski¹, H J Eckoldt², A Hauberg², S Lederer², L Lilje², T Wohlenberg², R Zimmermann² and A W Grau³

¹ European XFEL GmbH, Schenefeld, Germany

² DESY, Hamburg, Germany

³ Karlsruhe Institute of Technology, Karlsruhe, Germany

E-mail: johann.baader@xfel.eu

Abstract. The implementation and further improvements of superconducting undulators are part of the European XFEL facility development program. Within this program, a magnetic field test facility is being developed. Named SUNDAE2 (Superconducting UNDulator Experiment 2), it aims to perform in-vacuum magnetic field measurements of superconducting undulators (SCUs) with three techniques: Hall probe, moving wire, and pulsed wire. This contribution presents the updates and status of SUNDAE2.

1. Introduction

As part of the facility development program at European XFEL, a superconducting undulator (SCU) afterburner is foreseen to be installed directly at the exit of the already existing SASE2 hard x-ray permanent-magnet undulator (PMU) beamline. Six SCU modules — each with two 2 m-long superconducting undulator coils — are planned for the afterburner [1]. Initially, a pre-series prototype named S-PRESSO will be produced by Bilfinger Noell GmbH, delivered, and tested at European XFEL [2].

We are developing two SCUs test facilities for the undulators afterburner at European XFEL [3, 4, 5]. They are named SUNDAE1 and SUNDAE2 (Superconducting UNDulator Experiment). With SUNDAE2, we aim to perform in-vacuum magnetic field measurements of superconducting undulators (SCUs) using Hall probe [6], moving wire [7], and pulsed wire [8] techniques in the final cryostat. The pulsed wire and Hall probes are intended to measure the local magnetic field profile, while the moving wire measures the field integrals. This paper highlights the recent updates and status of SUNDAE2 developments.

2. S-PRESSO and vacuum chambers

Figure 1 shows the CAD design of S-PRESSO and the vacuum chambers that will encompass all the in-vacuum measurement systems. The whole infrastructure of SUNDAE1 and SUNDAE2 will be located in Hall 3 at DESY.



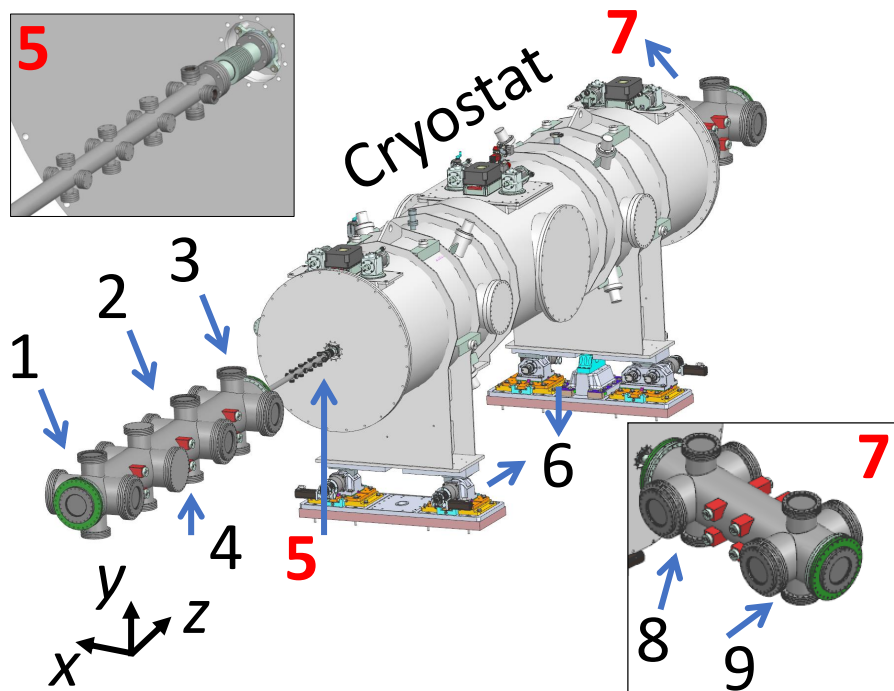


Figure 1. Sketch of SUNDAE2 vacuum chambers and S-PRESSO SCU module. Legend: (1) Region of Chamber 1 where the XY Ultra High Vacuum (UHV) translation stages are located. Stages are used for the Pulsed Wire System (PWS) and Moving Wire System (MWS). (2) Region of Chamber 1 where Hall Probe System (HPS) stepper motor and X (transversal) linear stage are. (3) Region of Chamber 1 where the parking position of the Hall probe carriage is located. (4) Space dedicated to collecting the wires from the HPS. (5) Viewports of Chamber 2 used to detect the wire displacement for the PWS. (6) Cam movers. (7) Chamber 3. (8) Region of Chamber 3 where HPS stepper motor and X linear stage are. (9). Region of Chamber 3 where the XY UHV translation stages are located (PWS and MWS).

A contract has been assigned to CECOM to produce the vacuum chambers. Due to potential welding issues close to the necks, the central tube will be increased to be compatible with DN350CF flanges¹. The total length, including the chambers and S-PRESSO, is 11 m.

S-PRESSO will have a 5 m-long cryostat with two 2 m-long SCU coils. The magnetic field period will be 18 mm, and the maximum on-axis peak magnetic field will be 1.82 T ($K_{\max} = 3.06$). The first and second field integral for both transversal field components have to be smaller than 4×10^{-6} Tm and 1×10^{-4} Tm², respectively. Made of copper, the beam chamber of S-PRESSO will have an elliptical shape with internal dimensions of 5 mm and 10 mm.

3. Pulsed and moving wire systems

The pulsed wire system (PWS) is regarded as a promising alternative to performing magnetic field measurements in undulators with limited accessibility (e.g., small gaps, in-vacuum/cryogenic environments, etc.). The technique was originally introduced by Warren [8]. The principle of the PWS is based on passing a current pulse through a stretched wire that crosses the magnetic field region, generating forces that produce an acoustic wave that travels along the wire. Depending on the shape of the pulse, the magnetic field or field integrals can be

¹ Initially, we considered a tube compatible with DN300CF flanges [5].

determined by detecting the wire displacement profile. An optical sensor measures the position of the wire as a function of time, which via post-process data techniques, can be converted into the magnetic field as a function of the longitudinal position.

The moving wire system (MWS) has demonstrated better performance to both the flipping coil and Hall probe techniques for measurements of field integrals [7]. It involves translating a wire inside the magnetic field and measuring the induced voltage. The technique requires having full control of the horizontal and vertical axis on both ends where the wire is fixed.

A single wire is planned for the pulsed and moving wire techniques in SUNDAE2. Two towers of Ultra High Vacuum (UHV) translation stages from SmarAct will be placed on the extremes of the chambers shown in Fig. 1 (see regions 1 and 9), which keeps a wire length of 10.5 m. The stages will carry out the required movement of the wire for field integral measurements and the wire positioning for the pulsed wire. The towers can stretch a wire up to 30 N. The absolute accuracy of the stages' positioning is better than 1 μm , and the reversal error and unidirectional repeatability are better than 0.5 μm . Nests, prisms, and reference pins are placed on both towers for the wire alignment. Counter-force springs are used to compensate for the weight of the elements on the brackets, allowing the Y stages to perform within their maximum lift force (1.5 N).

The high-power amplifier AeTechron 7234 will be used as the pulse generator. It has an output power of 900 W RMS. Figure 2 shows the preliminary test of the output current profile of amplitude 0.6 A and width of 100 μs in a BeCu wire with a length of 1.4 m and diameter of 125 μm . The input signal was generated from the RS PRO RSDG2122X waveform generator. Rise time is less than 2 μs , and over and undershoot is about 10%. Solutions to mitigate the over and undershoot effects are under investigation.

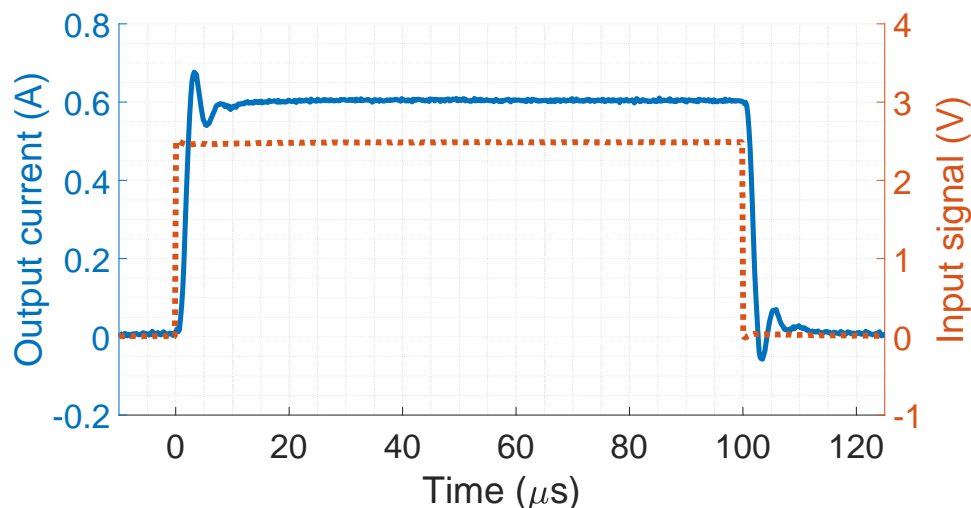


Figure 2. AeTechron 7234 test as a pulse generator.

The laser and photodetector will be placed out-of-vacuum to detect the wire displacement, close to the viewports of Chamber 2 (see inset 5 in Fig. 1). Such a concept must still be proved. Figure 3 shows a sensitivity measurement taken from the laser Thorlabs CPS532 and the photodetector Thorlabs PDA100A2 (the same BeCu wire with diameter of 125 μm was used) without viewports.

At the working point, a slope of 400 mV/ μm was obtained. It reliably detects a wire displacement of 0.1 μm over the noise. Considering the wire tested in the aforementioned measurements, a current of 1 A and tension of 15 N (both close to the maximum supported by the wire used in our tests), and with a pulse width of 10 μs (short pulse width for first field

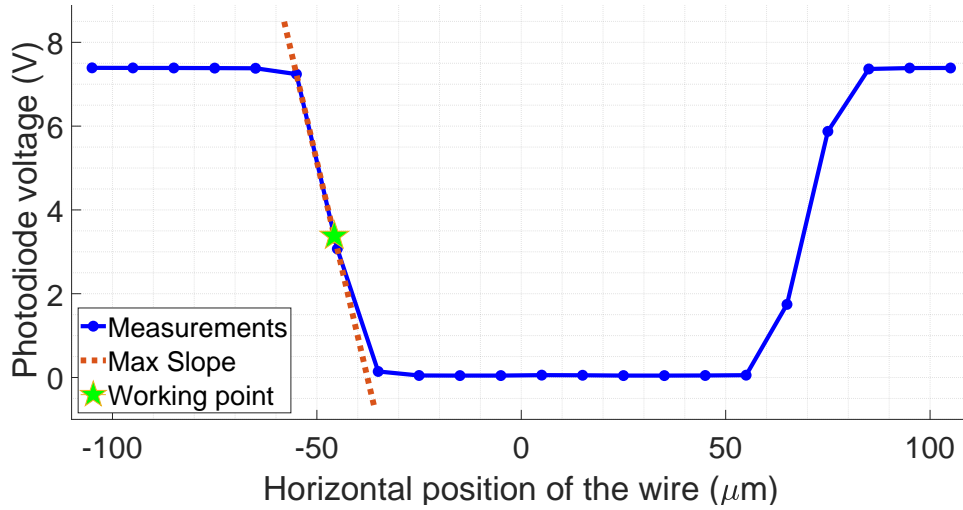


Figure 3. Pulsed wire system sensitivity measurements.

integrals), would give a displacement amplitude of $0.7 \mu\text{m}$ for the magnetic field profile designed for S-PRESSO. The estimated sag within the undulator is $200 \mu\text{m}$. It means a customized wire capable of supporting higher tension with a similar diameter may be needed to reduce the sag.

For the measurements with the PWS, dispersion will certainly dominate. We have developed a code that corrects dispersion based on algorithms proposed by Arbelaez *et al.* [9]. The corrections also include sag, finite pulse width, and discretization errors [10].

For field integral measurements with the MWS, the 8.5-digits precision digital multimeter (DMM) Agilent 3458A will take the voltage samples while the wire moves. Such DMM works with Power Line Cycles (PLC), which allows averaging out the 50 Hz noise from line cycle "pick-up" noise. Before and after the wire movement, a few voltage samples are taken to correct drifts and offsets linearly. Post-process data algorithms correct for the drift and offset, and calculate the integrated voltage numerically.

We plan to map field integrals with a wire displacement of 1 mm. A pre-amplifier would be required in this case; considering that we need to measure the first field integral better than $4 \times 10^{-7} \text{ Tm}$ (i.e., 1/10 of the maximum allowed first field integral), the DMM should be capable of detecting at least 0.4 nVs. Because of the small signals, we plan to integrate the EM DC A22 low-pass filter amplifier [11] into our system. The amplifier has demonstrated excellent performance for single-wire field integral measurements [12, 13].

4. Hall probe system

Primarily, Hall probes from Arepoc will be used. They were calibrated at Karlsruhe Institute of Technology (KIT). Figure 4 shows the calibration error² distribution of the same probe at three temperatures (4.2 K, 30 K, and 77 K). The standard deviation of all samples is approximately 0.15 mT.

Figure 5 presents the difference between calibration curves for 4.2 K, 30 K, and 77 K. The maximum error between fit curves is $\pm 0.4 \text{ mT}$ for $\pm 2 \text{ T}$.

An embedded 3-Axis Hall Magnetometer MagVector™ MV2 from Metrolab [14] will be tested at low temperatures. The dimensions of the probes ($3 \text{ mm} \times 3 \text{ mm} \times 0.9 \text{ mm}$) suit the limitations imposed by the beam chamber dimensions. Moreover, it would allow measuring more than one magnetic field component, which would be beneficial in terms of correcting the probes' position

² The difference between the high-order polynomial fit of the data points and NMR data points.

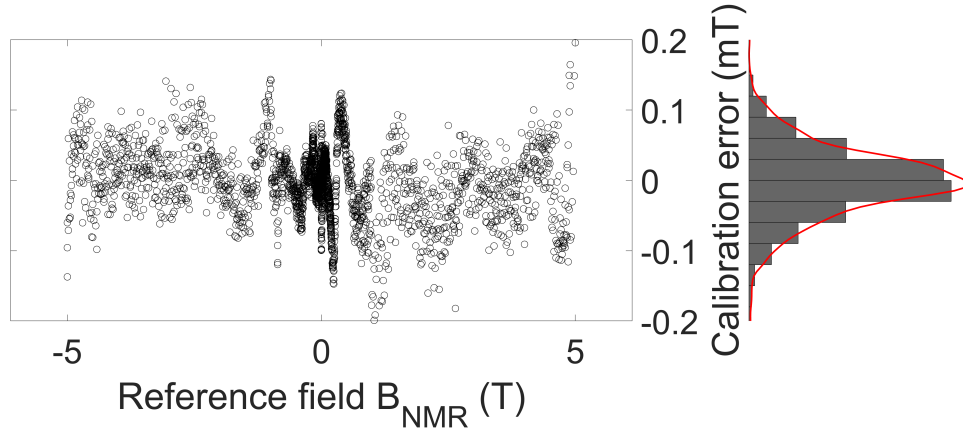


Figure 4. Calibration error *vs.* reference field.

on the carriage.

A carriage will incorporate three Hall probes to measure the vertical field component. We foresee one of them as a 3-Axis Hall probe to measure the horizontal field component. Figure 6 shows a prototype of the carriage with a length of 60 mm. A retroreflector will be set in one of the carriage's surfaces to measure the probes' longitudinal position with an interferometer. The carriage motion system is still under design.

Hall probes will be used in SUNDAE1 and SUNDAE2 test stands. For both, the Hall probes will be under cryogenic temperatures. Therefore, a test stand for calibration is required. A calibration stand is currently under development. It will be composed of a "cold finger" cryostat, an electromagnet model GMW 3474, and NMR sensors. The probe under calibration is set in a sample holder inside the cryostat. A set of goniometers control the cryostat position within the electromagnet gap. A second set of goniometers control the position of the NMR probes. Figure 7 illustrates the calibration stand concept.

The Hall probes used to measure the vertical component of SUNDAE2 will be placed at different heights. The relative vertical position of the probes' sensing area with respect to each

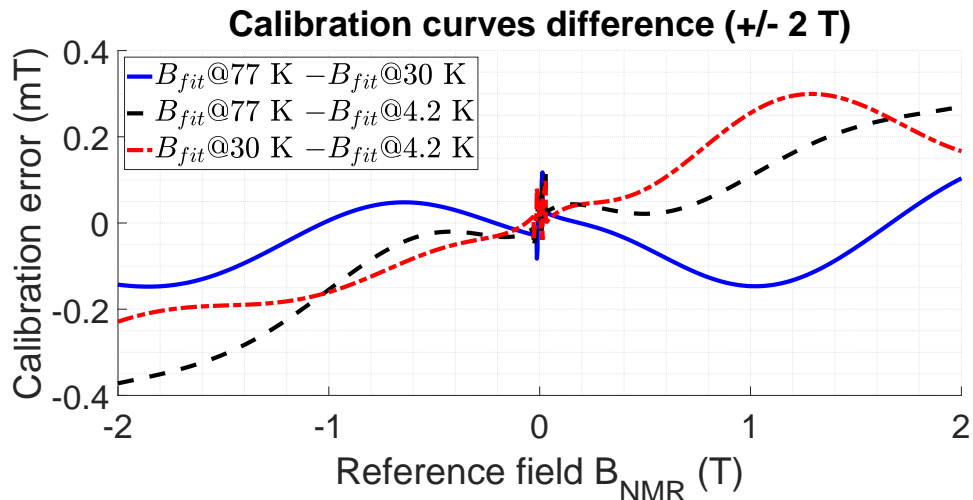


Figure 5. Calibration curve differences among three temperatures.

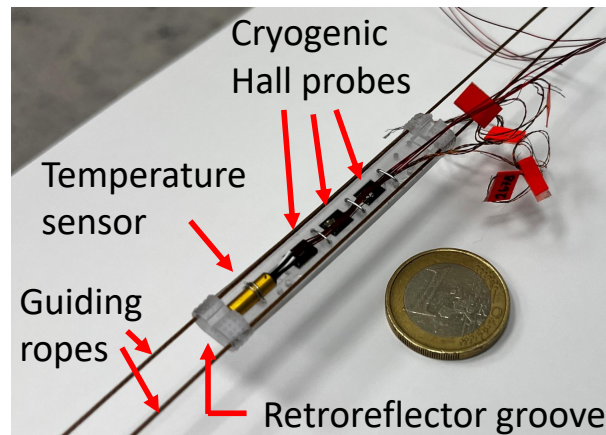


Figure 6. Hall probe carriage prototype.

other can be determined with the calibration test stand aforementioned. The goal of using three Hall probes is to fit the data from three different vertical positions (at the same longitudinal position) into $B = B_0 \cosh[2\pi(y - y_0)/\lambda_u]$, where B is the magnetic field measured with a probe, B_0 is the on-axis magnetic field, y_0 is the vertical position of the magnetic field axis, and λ_u is the undulator period. The fitting parameters are B_0 and y_0 . The variable λ_u is known from the magnetic field measurements *vs.* the probe's longitudinal position taken from the interferometer. Simulations showed that B_0 can be recovered with an uncertainty of ± 0.1 mT.

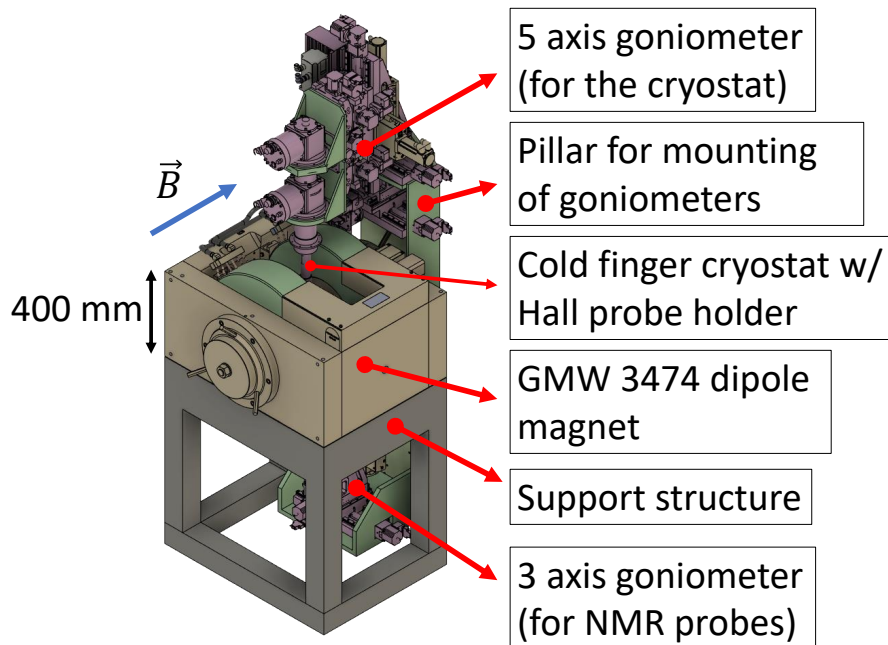


Figure 7. Hall probe calibration test stand concept.

Acknowledgments

This project has partially received funding from the European Union's Horizon 2020 research and innovation programme under grant agreement No 101004728 (LEAPS-INNOV).

References

- [1] Casalbuoni S *et al.* 2022 *Proc. IPAC'22* pp 2737–2740 URL <https://doi.org/10.18429/JACoW-IPAC2022-THPOPT061>
- [2] Casalbuoni S *et al.* 2022 *J. Phys.: Conf. Series* **2380** 012012 URL <https://dx.doi.org/10.1088/1742-6596/2380/1/012012>
- [3] Marchetti B *et al.* 2022 *J. Phys.: Conf. Series* **2380** 012027 URL <https://dx.doi.org/10.1088/1742-6596/2380/1/012027>
- [4] Marchetti B *et al.* 2022 *Proc. IPAC'22* pp 2646–2648 URL <https://doi.org/10.18429/JACoW-IPAC2022-THPOPT031>
- [5] Baader J *et al.* 2022 *Proc. IPAC'22* 13 pp 2649–2652 URL <https://doi.org/10.18429/JACoW-IPAC2022-THPOPT032>
- [6] Sanfilippo S 2009 *CERN Accelerator School CERN-2010-004* pp 423–462
- [7] Zangrando D and Walker R P 1996 *Nucl. Instrum. Methods Phys. Res. A* **376** 275–282 URL [https://doi.org/10.1016/0168-9002\(96\)00207-0](https://doi.org/10.1016/0168-9002(96)00207-0)
- [8] Warren R 1988 *Nucl. Instrum. Methods Phys. Res. A* **272** 257–263 URL [https://doi.org/10.1016/0168-9002\(88\)90233-1](https://doi.org/10.1016/0168-9002(88)90233-1)
- [9] Arbelaez D, Wilks T, Madur A, Prestemon S, Marks S and Schlueter R 2013 *Nucl. Instrum. Methods Phys. Res. A* **716** 62–70 URL <https://doi.org/10.1016/j.nima.2013.02.042>
- [10] Baader J E and Casalbuoni S 2022 *Measurement* **193** 110873 URL <https://doi.org/10.1016/j.measurement.2022.110873>
- [11] EM Electronics <http://www.emelectronics.co.uk/low-level-dc-voltage-amplifier-modules/em-dc-amplifier-model-a22/>, [Online; accessed March 13th, 2023]
- [12] Baader J 2019 *Proc. FEL'19* pp 484–487 URL <https://doi.org/10.18429/JACoW-FEL2019-WEP067>
- [13] Wolf Z 2022 *22nd Int. Magnetic Measurement Workshop (IMMW22)*
- [14] Metrolab MagVector™ MV2 Magnetometer <https://www.metrolab.com/products/magvector-mv2/>, [Online; accessed March 9th, 2023]